COMPUTER SIMULATION OF THE EXTENDED OBJECT IMAGE FORMATION THROUGH TURBULENT ATMOSPHERE. PART II. ALGORITHM AND EXAMPLES

V.P. Kandidov, S.S. Chesnokov, and S.A. Shlenov

M.V. Lomonosov State University, Moscow
Received May 13, 1997

We propose an algorithm for direct computer simulation of random samples of the image of an incoherently illuminated object that is viewed through the atmospheric layer. The algorithm has been constructed based on the method developed in Ref. 1. This algorithm can be used in the development and tests of image processing methods, simulation of adaptive systems of image correction, and in other problems.

The image transfer simulator developed in Ref. 1 assumes the use of anisoplanatic systems what is common for the problems of vision through the turbulent atmosphere. It is clear that for such systems it is impossible to introduce the optical transfer function (OTF) since every fragment of an extended object image is distorted, generally speaking, differently than other ones. Therefore we propose that the algorithm to obtain a realization of a short-exposure image be based on the superposition integral of random short-exposure point spread functions (PSF) $\tilde{S}_{\exp}(\mathbf{r}, \mathbf{r}', \eta)$. As shown in Ref. 1 PSF $\tilde{S}_{\exp}(\mathbf{r}, \mathbf{r}', \eta)$ may be represented as $\tilde{S}_{\exp}(\mathbf{r}, \mathbf{r}', \eta) = S_{0S}(\mathbf{r} - \xi - \tilde{\xi}(\mathbf{r}', \eta))$, where the PSF S_{0S} describes the spread due to diffraction, due to averaged contribution from small-scale fluctuations, and because of random displacements $\tilde{\xi}(\mathbf{r}', \eta)$ of the spreaded point centers from their geometric optical positions; $\xi(\mathbf{r}') = -M\mathbf{r}'$ are determined by large-scale fluctuations.

1. ALGORITHM OF COMPUTER SIMULATION OF AN IMAGE RANDOM REALIZATION

In accordance with the above-said the algorithm developed includes the following basic stages:

1. Calculation of the PSF $S_{0S}(\mathbf{r} - \xi)$ that determines the point image spread due to diffraction and averaged contribution from small-scale fluctuations for a preset parameters of an atmospheric path and the image forming optics. To do this, we make use of the isoplanatism property of the subsystem with the averaged PSF. According to this property, $S_{0S}(\mathbf{r})$ is a result of the inverse Fourier transform from OTF of this subsystem $S_{0S}(\mathbf{r}) = F^{-1}\{H_{0S}(\Omega)\}$.

2. Determination of the random displacements of the object's point images $\tilde{\xi}(\mathbf{r}', \eta)$ based on the model of a single phase screen.

3. Calculation of the random intensity distribution $\tilde{I}(\mathbf{r})$ over the image which is a superposition of the PSF $S_{0S}(\mathbf{r})$ taken with the point intensity weights $I(\mathbf{r}')$ and displaced by the random value $\tilde{\xi}(\mathbf{r}', \eta)$ from the image geometric position of these points $\xi(\mathbf{r}')$.

2. RANDOM DISPLACEMENTS OF OBJECT POINTS

Determination of the random displacements $\tilde{\xi}(\mathbf{r}', \eta)$ of object point images is based on the model of a single phase screen for the turbulent atmosphere. Then we calculate the wave-front tilt $\tilde{\theta}(\mathbf{r}', \eta)$ introduced by the phase screen region that determines the formation of the object point $\mathbf{r}'$ image. Such a region is separated out by a cone with a vertex at the object point $\mathbf{r}'$ and the base coinciding with a lens aperture having the diameter d (see Fig. 1*a*). The wave-front tilt $\tilde{\theta}(\mathbf{r}', \eta)$ is a random function of the coordinate $\mathbf{r}'$ (see Fig. 1*b*). Correlation function of tilts, $\langle\tilde{\theta}(\mathbf{r}')\,\tilde{\theta}(\mathbf{r}' + \delta\mathbf{r})\rangle$, is determined by statistical properties of the phase screen simulating the atmospheric turbulence. For the statistically independent short-exposure realizations of the image the tilt $\tilde{\theta}(\mathbf{r}')$ should satisfy the condition

$$\langle\tilde{\theta}_j(\mathbf{r}')\,\tilde{\theta}_{j'}(\mathbf{r}')\rangle = \sigma_\theta^2\,\delta_{jj'}, \qquad (1)$$

where j, j' are the realization numbers; σ_θ^2 is the variance of wave-front tilts.

In the case of a moving phase screen simulating the wind drift of the turbulence the tilt $\tilde{\theta}(\mathbf{r}', \eta)$ also depends, in a random way, on the slow time η. In accordance with the hypothesis of the "frozen" turbulence for the tilt $\tilde{\theta}(\mathbf{r}', \eta)$ the following relation is true:

0235-6880/98/05 451-05 $02.00

$$\tilde{\theta}(\mathbf{r}', \eta + \eta_0) = \tilde{\theta}\,[\mathbf{r}' - (V/2)\eta_0, \eta]. \quad (2)$$

Hereby the spatiotemporal correlation of the wave-front tilts is set for different points of the object.

The tilt $\tilde{\theta}(\mathbf{r}', \eta)$ is determined by two components, $\tilde{\theta}_x(\mathbf{r}', \eta)$ and $\tilde{\theta}_y(\mathbf{r}', \eta)$, in the planes *XOZ* and *YOZ*, respectively. Since the region diameter $d/2$ is much smaller than the characteristic dimension of large-scale inhomogeneities the components $\tilde{\theta}_x$ and $\tilde{\theta}_y$ can be calculated as the ratios of the phase difference on the boundaries of the region separated out to $d/2$ (see Fig. 1*b*)

$$\tilde{\theta}_x = \frac{\tilde{\varphi}_x^+(\mathbf{r}', \eta) - \tilde{\varphi}_x^-(\mathbf{r}', \eta)}{k\,d/2};$$

$$\tilde{\theta}_y = \frac{\tilde{\varphi}_y^+(\mathbf{r}', \eta) - \tilde{\varphi}_y^-(\mathbf{r}', \eta)}{k\,d/2}. \quad (3)$$

Here $k = 2\pi/\lambda$; $\tilde{\varphi}_x^+$ and $\tilde{\varphi}_x^-$ are the values of phase fluctuations on the diameter of the region separated out that is parallel to the plane *XOZ*, and $\tilde{\varphi}_y^+$, $\tilde{\varphi}_y^-$ are the values of phase fluctuations on the diameter *YOZ*.

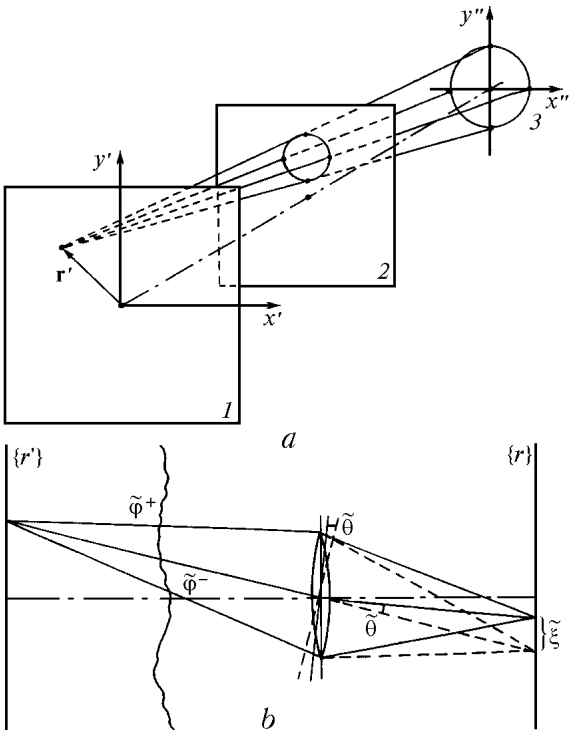

FIG. 1. Determination of random displacements of the object's points: the phase screen region influencing the point image position (a), calculation of the random tilt $\tilde{\theta}$ *and displacement* $\tilde{\xi}$ *for a point image (b),* φ^+ *and* φ^- *are the values of phase fluctuations on the ends of the diameter of the phase screen region.*

The components $\tilde{\xi}_x(\mathbf{r}', \eta)$ and $\tilde{\xi}_y(\mathbf{r}', \eta)$ of the vector of random displacement $\tilde{\xi}(\mathbf{r}', \eta)$ of the point image with the coordinate $\mathbf{r}'$ equal to

$$\tilde{\xi}_x(\mathbf{r}', \eta) = \tilde{\theta}_x(\mathbf{r}', \eta)\, f,$$
$$\tilde{\xi}_y(\mathbf{r}', \eta) = \tilde{\theta}_y(\mathbf{r}', \eta)\, f. \quad (4)$$

3. GRID IN THE OBJECT PLANE

For computer simulation the two-dimensional fields of the object intensity $I(\mathbf{r}')$, image intensity $\tilde{I}(\mathbf{r})$, phase fluctuations $\tilde{\varphi}$, the angular displacements $\tilde{\theta}(\mathbf{r}', \eta)$, and of the spatial ones $\tilde{\xi}(\mathbf{r}', \eta)$ are presented on discrete grids in the corresponding planes which are perpendicular to the axis *OZ*. The choice of optimal parameters of these grids, in the first place the digitization step h, is most important in development of an effective computer code to construct images.

To estimate the grid step h' in the plane $\{\mathbf{r}'\}$, we make use of the properties of the diffraction-limited noncoherent optical system. The OTF $H_0(\Omega)$ and PSF $S_0(\vartheta)$ of such a system[2] are presented in Fig. 2, where Ω_0 is the cuttoff frequency of the noncoherent optical system, ϑ_0 is the angle width of the PSF. For ϑ_0 and linear width of the PSF in the object plane Δr_0 it is valid that

$$\vartheta_0 = \lambda/d, \quad \Delta r_0 = z\,\vartheta_0. \quad (5)$$

For the grid in the object plane $\{\mathbf{r}'\}$ with the step h' the corresponding angular step is

$$\Delta\vartheta = h'/z. \quad (6)$$

Nyquist frequency Ω_N for it equals

$$\Omega_N = 1/(2\Delta\vartheta). \quad (7)$$

According to the sampling theorem[3] a function with a bounded spectrum of half width Ω_0 is accurately reproduced on a grid if its Nyquist frequency satisfies the condition

$$\Omega_N \geq \Omega_0. \quad (8)$$

The inequality sign in condition (8) corresponds to a redundant grid. The OTF and PSF for this grid are presented in Fig. 2*b*. For a limited number of the grid nodes M the grid with the Nyquist frequency $\Omega_N = \Omega_0$ is optimal. Hence the optimal step by angle equals

$$\Delta\vartheta_{\text{opt}} = \lambda/(2d). \quad (9)$$

The OTF $H_0(\Omega)$ and PSF $S_0(\vartheta)$ for an optimal grid are presented in Fig. 2*a*.

Under conditions of small-scale phase fluctuations the cuttoff frequency Ω_0 of a noncoherent optical system does not increase and the condition (8) is not violated. According to this fact the PSF of that system $S_{0S}(\theta)$ can not become narrower because of the averaged contribution from the small-scale fluctuations.

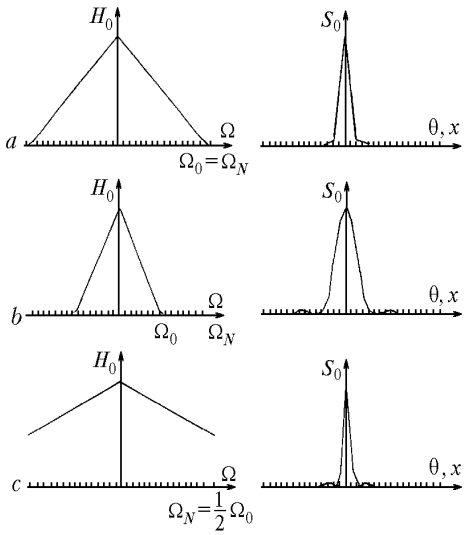

FIG. 2. The OTF $H_0(\Omega)$ and PSF $S_0(x)$ of a diffraction-limited noncoherent optical system presented on the calculation grid; $x = \vartheta f$, Ω_N is the Nyquist frequency of the grid, Ω_0 is the optical system cuttoff frequency: the optimal grid for $\Omega_N = \Omega_0$ (a), the redundant grid for $\Omega_N > \Omega_0$ (b), the grid does not represent the diffraction spread at $\Omega_N < \Omega_0$ (c).

The diffraction spread of a point is not reproduced identically on a grid with the angular step $\Delta\vartheta < \Delta\vartheta_{opt}$ and, therefore, the Nyquist frequency $\Omega_N < \Omega_0$. In particular, for $\Delta\vartheta = 2\Delta\vartheta_{opt}$ or $\Omega_N = 0.5\Omega_0$ the diffraction spread of a point vanishes (Fig. 2*c*).

4. ILLUSTRATION OF THE ALGORITHM

The algorithm discussed above is illustrated in Figs. 3 and 4, where the single realizations of the short-exposure images and "long-exposure" images, averaged over $M = 20$ realizations of independent phase screens, of the test objects are presented. The results have been calculated on a 128 by 128 grid with the optimal step.

Figure 3 presents the images of points of the object that consists of four point sources placed at the vertices of a square. One can see that the point images are spread by the diffraction and small-scale inhomogeneities equally. It is also seen from this figure that in every realization of the large-scale inhomogeneities these images are being independently shifted relative to each other. Centers of the averaged images are close to the geometric optical images of the object points.

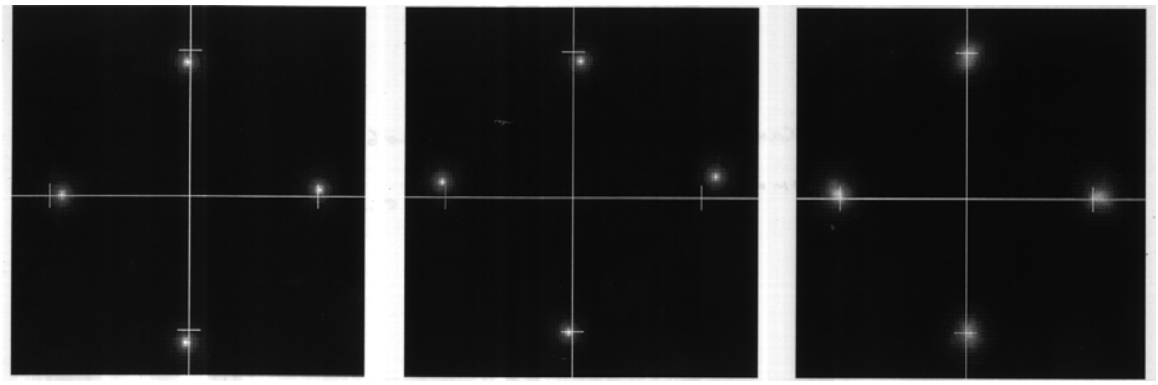

FIG. 3. Image of the test-object consisting of four luminous points observed through the turbulent atmosphere: two realizations of short-exposure images (a, b), the image averaged over 20 realizations (c). Geometric optical positions of the point images are marked by notches on the coordinate axes. Conditions of the numerical experiment: $\lambda = 0.5$ μm, $C_n^2 = 5\cdot10^{-16}$ cm$^{-2/3}$, $L = 64$ cm, $d = 10$ cm, $z = 2$ km, *grid dimension is* 128×128, *the grid step in the object plane* $h' = 0.5$ cm.

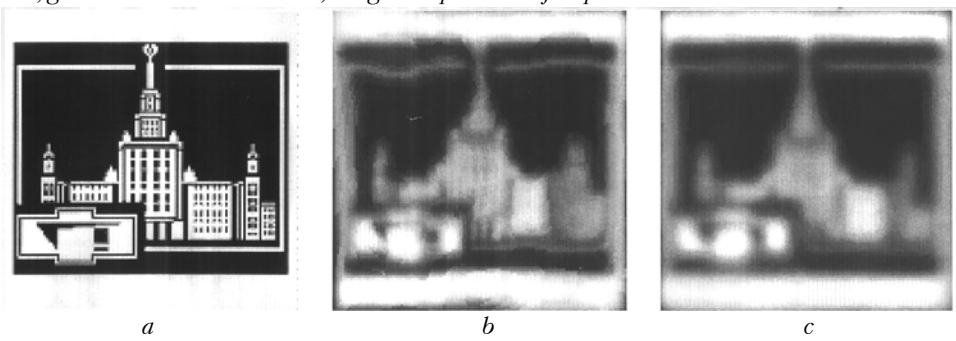

FIG. 4. Illustration of the algorithm of the image distortions simulation: the object (a), one realization of a short-exposure image (b), the image averaged over 20 realizations (c). Conditions of the numerical experiment are the same as in Fig. 3.

One may judge on the capabilities of the algorithm of simulating the images of complex two-dimensional objects by an example presented in Fig. 4 (the emblem of Moscow State University viewed through a two-kilometer thick atmospheric layer).

5. EFFECTIVE FRIED RADIUS

As was mentioned, the general idea of the simulator developed consists in that the influence of small-scale turbulence is described by the averaged OTF $H_{0S}(\Omega)$, whereas the large-scale inhomogeneities are simulated by generating the phase screens with the subsequent separation of random wave-front tilts. Such an approach provides for the account of a wide range of the refractive index fluctuations within the limits of a single problem, but it requires to agree the parameters of both components of the image transfer simulator. The basic parameter that characterizes the averaged spread of images by the small-scale turbulence is the Fried radius r_0 entering into the expressions (15) and (23) from Ref. 1. To agree both simulator components, we shall obtain the effective Fried radius r_{ef} for the averaged distortions introduced by a phase screen. In this case we use a parametric expression for the long-exposure OTF, $H_L(\Omega)$

$$H_L(\Omega) = \exp\{-3.44\,(\lambda\Omega / r_{ef})^c\}. \qquad (10)$$

Here the power index c and the effective radius r_{ef} are unknown constants. To obtain this constants, we use the phase screen method and perform the series of numerical experiments to determine the average OTF $H_L(\Omega)$. In this case we shall assume that the basic contribution into the distortions is introduced by the random wave-front tilts at the lens aperture.

In the numerical experiments we have many times generated realizations of the random phase screens for the preset parameters of the atmospheric turbulence. Calculation of the phase difference $\Delta\tilde{\varphi}_i$ on the diameter of the region separated out was performed for every phase screen on the uniform grid on object with the dimension L. Further, the random deviation $\tilde{\theta}_i$ of the wave-front tilt angle behind a lens was determined by the following formula:

$$\tilde{\theta}_i = [\lambda / (2\pi d)]\,\Delta\tilde{\varphi}_i. \qquad (11)$$

Histogram of the obtained angle deviations $\tilde{\theta}_i$ was interpreted as the averaged long-exposure PSF $S_L(\mathbf{r})$. The long-exposure OTF $H_L(\Omega)$ was obtained from $S_L(\mathbf{r})$ by the Fourier transform. Then by the method of least squares the parameters c and r_{ef} of thus simulated OTF were determined. A run of numerical experiments to obtain the Fried effective radius for different parameters of the atmospheric turbulence was performed on the grid with the node number $N \times N = 128 \times 128$, the lens diameter $d = 5$ cm, and the object dimension $L = 5$ m. In every numerical experiment the realization number was $M = 10$ of independent phase screens. The Kolmogorov model of the atmospheric turbulence was used.

It should be noted that the power index c practically does not differ from the value $c \approx 2$. This fact shows that calculations of the PSF were made only with the account of wave-front tilts. Weak dependence of r_{ef} on the lens diameter d and grid dimension N has been established in these simulations. Thus, when the lens diameter d changes from 1 to 50 cm, that is by 50 times, the parameter r_{ef} changes no more than by 50%. This circumstance allows us to consider only one value of r_{ef}.

When the number of the calculation grid nodes on the phase screen grows a tendency to decreasing difference between values of r_{ef} and r_0 is observed. This fact is connected with better representation of the atmospheric turbulence structure on the phase screens with large number of nodes. However, as numerical experiments showed, the essential differences of r_{ef} from r_0 can be observed on the grids with $N = 128$ that are often used in practice. The Fried radius r_0 has been changed from 0.2 to 33 cm in the series of experiments performed. For every value r_0 the effective Fried radius r_{ef} was determined from the experiments. Analysis of the obtained data allowed us to derive an analytical dependence of r_{ef} on r_0 in the form of the following approximation formula:

$$r_{ef} = 1.82\, r_0^{0.83}, \qquad (12)$$

In this case the value r_0 in (12) should be in centimeters. For $N = 128$ the formula (12) approximates the values r_{ef} obtained in the experiments with the accuracy better than 1.4% over the entire region $0.2 \le r_0 \le 33$ cm.

6. CONCLUSION

The algorithm proposed in this paper has been realized in the form of specialized subroutines for the IBM-compatible computers. The user interface running in the Windows 3.1 and Windows–95 environment has been developed also. This interface allows one to easily change the parameters of numerical experiments and observe, on a display, the dynamic distortions of images as well as of the averaged (long-exposure) ones. Initial distributions of light intensity in the object plane, which are the input data for the computer simulation, are entered into a computer memory in the Windows Bitmap format. The output data are a sequence of the two-dimensional arrays describing short-exposure intensity distributions in the image plane with some step in time.

The data obtained on the basis of the developed algorithm can be used to develop and test algorithms of image processing, simulate adaptive systems for image correction, and also for other model problems in applied optics.

ACKNOWLEDGMENT

The authors are grateful to N.G. Iroshnikov for his valuable contribution to the development of the user's interface.

REFERENCES

1. V.P. Kandidov, S.S. Chesnokov, and S.A. Shlenov, Atmospheric and Oceanic Optics **11**, No. 4, 349–352 (1998).

2. D. Goodman, *Introduction to Fourier Optics* (McGraw Hill, New York, 1968).

3. L. Rabiner and B. Gould, *Theory and Application of Digital Processing of Signals* [Russian translation] (Mir, Moscow, 1978), 848 pp.